Addressing individual paramagnetic molecules through ESN-STM

M. Mannini [a,*], P. Messina [a], L. Sorace [a], L. Gorini [a], M. Fabrizioli [a,b], A. Caneschi [a], Y. Manassen [c], P. Sigalotti [d], P. Pittana [b], D. Gatteschi [a]

[a] *Department of Chemistry and INSTM Research Unit, University of Florence, Via della Lastruccia 3, 50019 Sesto Fiorentino, Italy*
[b] *Sincrotrone, Science Park Area, Campus Basovizza, 34012 Trieste, Italy*
[c] *Department of Physics, Ben Gurion University of the Negev, P.O. Box 653, Beer Sheva 84105, Israel*
[d] *APEResearch, Science Park Area, Campus Basovizza, 34012 Trieste, Italy*

Abstract

We present our recent efforts in the build-up of a room temperature electron spin noise scanning tunnelling microscope (ESN-STM) designed for ultra-thin molecular films investigation. We describe here the first results obtained with this system on a commercial paramagnetic molecule deposited on Au(111) surfaces, namely 1,1-diphenyl-2-picrylhydrazyl (DPPH). Further we briefly present our ongoing work on the preparation and characterization of a new class of samples for this instrumentation. These are based on the self-assembling on surfaces of functionalized organic radicals. We suggest here a complete procedure to assess a good candidate molecule for ESN-STM experiments through X-band CW-ESR, standard STM investigations and ToF-SIMS analysis.
© 2007 Elsevier B.V. All rights reserved.

Keywords: ESN; STM; ESR; Organic radicals; Ultrathin films

1. Introduction

The increasing interest in the detection of a single electron spin is due to the possibility of addressing the physical properties of a single molecule. STM techniques have pushed the spatial resolution limit to atomic size, but single spin sensitivity is still a hard challenge. The combination of single spin sensitivity and sub nanometer spatial resolution would allow a sensible scale down of existing memory devices. It also would be extremely relevant to the use of a single spin as a qubit for quantum computation, information and spintronics [1]. All such issues are central goals in nano-scale science and technology.

One of the most promising techniques for single spin detection is the ESN-STM technique, which is based on the detection of spin noise in the tunneling current of the STM experiment at the Larmor frequency of the spin. This technique has been first described and proved to be effective more than a decade ago by one of the authors [2]. These measurements exploit the unparalleled spatial resolution of the scanning tunneling microscope (STM) to locate the individual spin centers on a surface. ESN-STM features a sensitive RF recovery system for detecting very low RF power signals in the tunnelling current, a permanent magnet in order to apply a DC field of several hundreds Gauss, coils for phase sensitive detection and RF filters.

Recent results have proven that electron spin noise induced oscillations at the Larmor frequency in the tunnelling current detected by STM. ESN-STM signal can be detected not only in dangling bonds at silicon surfaces as originally demonstrated [2], but also looking at organic radicals deposited on surfaces [3].

ESN-STM is also known as electron spin resonance (ESR)-STM. Indeed even if there is no effective resonance

---

* Corresponding author. Tel.: +39 0554573327; fax: +39 0554573372.
E-mail address: matteo.mannini@unifi.it (M. Mannini).

(as no energy is pumped into the system), ESN-STM locally exploits the same observable recovered as average value in standard ESR measurement, i.e. the precession frequency of the electron spin under the action of a static magnetic field.

We describe here our home built ESN-STM setup and we report the verification of these recent results using a different organic radical, DPPH, as discussed elsewhere [4]. We describe also our ongoing work focused on the preparation and characterization of a new class of samples based on the use of nitronyl nitroxide radicals appropriately engineered for gold surface deposition and self-assembling. These can serve as bench test for the ESN-STM technique.

2. ESN-STM instrumentation

The ESN-STM apparatus is a room temperature STM which features a high shielding of external RF noise, the possibility of applying an external (DC and AC) magnetic field and the presence of an RF detection system. The tunnelling current coming out from the usual tunnelling junction formed between the sample and the metallic tip of the microscope is split into two channels. The first acquires the DC component with a conventional current-voltage converter for the STM imaging through the distance control feedback circuit. The second one collects the AC component to be analyzed by an RF amplifier. In order to enhance the sensitivity to weak signals, this amplifier is inserted inside the STM head.

We have used a general protocol (proposed by one of the authors) to detect the low level RF signal from the STM tip [5]. The scheme of this apparatus is illustrated in Fig. 1. A small oscillating magnetic field is added to a static magnetic field so that the resulting magnetic field on the sample surface is modulated along the direction of the static field: $B = B_0 + \Delta B \cos(\omega_m t)$. Here, ω_m is the modulation frequency and $2\Delta B$ is the peak-to-peak intensity of the modulation. The signal is extracted from the tunnelling current as a power peak in the spectral density occurring at the Larmor frequency $\upsilon_L = \omega/2\pi = g\mu_B B/h$ (where μ_B is the Bohr magneton and h the Planck's constant) which is modulated at ω_m. The frequency at which the signal is observed depends on the g factor of the spin center, on the applied field B and on the modulation frequency of the oscillating field ω_m. It can be expressed as

$$\omega(t) = \omega_0(t, T_1) + \Delta\omega \cos(\omega_m t + \phi(t, T_2))$$

where ω_0 is the unmodulated frequency, ϕ is the phase and $\Delta\omega = g\mu_B\Delta B/\hbar$ is the frequency modulation intensity, where both ω_0 and ϕ are unknown functions of time. The former depends on the hyperfine interaction, the g-anisotropy and the longitudinal relaxation time T_1, while the latter is determined by the transverse relaxation time T_2 [5].

The Fourier transform of such a signal, obtained by a spectrum analyser will give a typical sideband spectrum structure constituted by a set of equally spaced sidebands
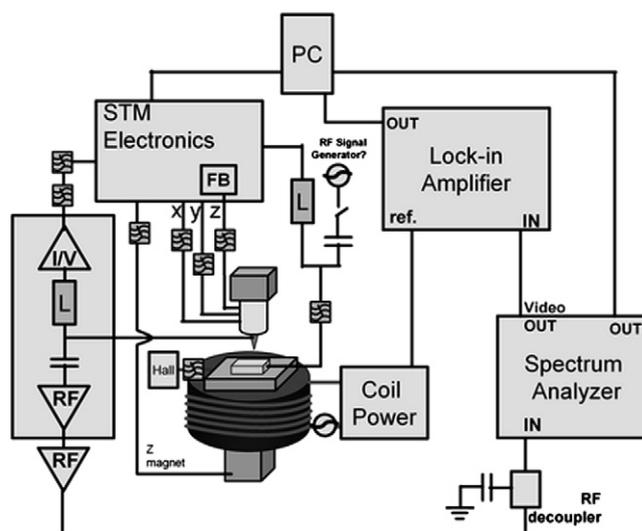

Fig. 1. Detection scheme for ESN-STM. The signal, modulated by superimposing an oscillating magnetic field over a static one on the sample surface, is recovered from the STM tunnelling current by splitting it into a low frequency and a high frequency part: the latter is then amplified and processed by a spectrum analyzer and signal extraction is finally improved by means of phase sensitive detection.

with frequencies $(\omega_0 \pm n\omega_m)$ and with intensities of $J_n(m_\omega)$ where J_n is the nth-order Bessel function of the first kind and $m_\omega = \Delta\omega/\omega_m$ is the modulation index corresponding roughly to the maximum value of n, so that the total width of the spectrum equals to $2\Delta\omega$. The best sensitivity is obtained by setting the modulation index equal to 2, so as to maximize the J_1 component of the Fourier spectrum, and making use of a lock-in amplifier referenced to ω_m to exploit PSD. An additional consideration is that, in order to ensure maximum modulation, the bandwidth of the detector has to be of the same order of magnitude of the modulation intensity.

We termed this technique *electron spin noise* spectroscopy [5,6]: the fluctuation of the single spin is basically detected as an incoherent phenomenon, like in *nuclear spin noise* spectroscopy [7].

3. Preparation of DPPH samples

All the samples investigated are prepared exploiting the self-assembling of monolayer technique [8] or a similar approach in which the key steps are the adsorption and the removal of the excess of deposited molecules via cleaning with solvents. The latter step is effective as long as intermolecular interactions are weak. This allows one to obtain monolayer or submonolayer coverage of the metallic surface, by varying exposure times.

Samples for ESN-STM were prepared by immersing a flame annealed Au(1 1 1) 150 nm thick film evaporated on mica into CH_2Cl_2 solutions of 1,1-diphenyl-2-picrylhydrazyl (DPPH) (purchased from Sigma Aldrich, Inc.). The solution concentration has been varied from 0.1 to 0.01 mM and the exposure time from 1 min to

15 min in order to optimize the deposition process. The sample was then rinsed 3/4 times for 10–30 s into pure CH_2Cl_2, and dried under nitrogen fluxing.

For DPPH, as already reported for α,γ-bisdiphenylene-β-phenylallyl (BDPA) [3a], the adsorption on the gold surface occurs as a consequence of stacking interactions between the delocalized π-orbitals of the aromatic rings and the delocalized surface electrons of the gold surface. These interactions are reasonably stronger than those between molecules decreasing the possibility of clustering of molecules over the surface. Clustering was observed via STM investigation only for longer exposure time.

4. CW-ESR characterization of DPPH samples

In order to have independent information on the layers, standard CW-ESR experiments can be performed. However, it must be remembered that this approach suffers from the fact that in bulk ESR spectroscopy a signal averaged over a large number of molecules and depending on intermolecular interactions is obtained, while ESN-STM is sensitive to the paramagnetism of just one molecule.

CW-ESR spectra were recorded using a Bruker Elexsys E500 spectrometer working at X-band ($v \sim 9.4$ GHz) equipped with a SHQ cavity. Ultrathin film samples for investigation with this technique were obtained by incubating Au(1 1 1) flame annealed slides for 4 h in 0.1 mM CH_2Cl_2 solutions 0.1 mM solutions of the radicals.

Continuous wave ESR (CW-ESR) measurements on DPPH films proved that these molecules retain their paramagnetic character on the Au(1 1 1) surface (Fig. 4).

The ESR spectrum shows a single line with $\Delta H_{pp} = 2.8$ G (Fig. 2a). No hyperfine structure is observed, in contrast with solution spectrum, showing the expected five lines pattern due to the hyperfine coupling with two almost equivalent ^{14}N $I = 1$ nuclei (coupling with ^1H being unresolved). Compared to a standard solid sample the linewidth is broader (4 G compared to 1 G) and indicates an incomplete exchange narrowing process. This suggests that the

molecules are close enough to interact between themselves [9], possibly indicating the formation of small molecular aggregates of DPPH.

5. ESN-STM of DPPH samples

In order to rule out the presence of spurious noise signals in the ESN-STM experiment, the first necessary test is the collection of a series of spectra without approaching the STM tip to the surface. Furthermore the RF detection setup is checked by introducing an external RF signal of intensity comparable to the expected one.

After having successfully accomplished these tests, real measurements are performed in tunnelling conditions. The first step consists of a standard STM characterization of the sample aimed at finding the best imaging conditions and checking the quality of the molecular film.

Fig. 3a shows typical images observed for DPPH molecules deposited on Au(1 1 1) surfaces. As the geometrical size of the smallest white spots corresponds to DPPH molecular size within the experimental error, we attribute them to single molecules. Larger white spots indicate the formation of agglomerates of two or few molecules.

Spin noise measurements are then performed when isolated molecules or at least small cluster of molecules are identified. ESN-STM signals reported herein were obtained by collecting noise spectra during scanning. Only 0.5% of the sampling give a real signal with respect to the noise, a behaviour which we attribute to the elusive characteristics of the signal [4]. Indeed, for a signal to be detected it is necessary that it exists at a given frequency for the entire duration in which the narrow band detector samples the signal; this condition might be difficult to achieve for molecules with largely spreading hyperfine sublevels. Notwithstanding these inherent limitations, signals coming from single molecules can be detected as shown below here and in previous papers [2–5].
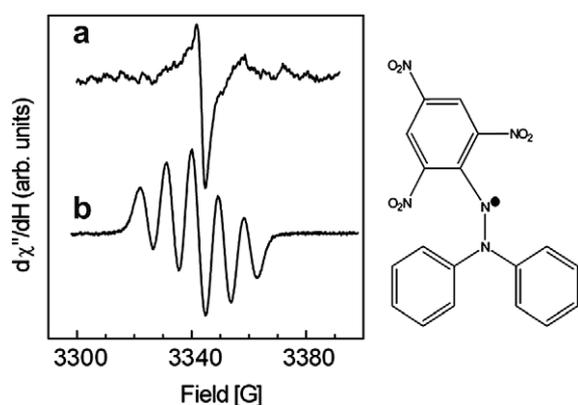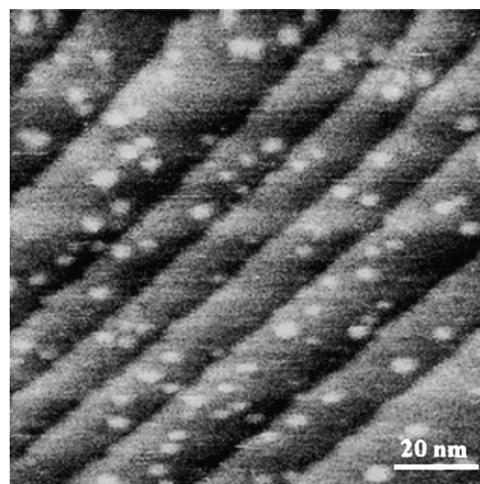
Fig. 2. Room temperature CW-ESR spectra of DPPH (molecule sketched on the right) (a) as ultrathin film sample and (b) 0.1 mM dichloromethane solution.

Fig. 3. STM image of DPPH molecules deposited on Au(1 1 1). Tunnelling current (I_t): 10 pA, Bias voltage (BV): 0.1 V.
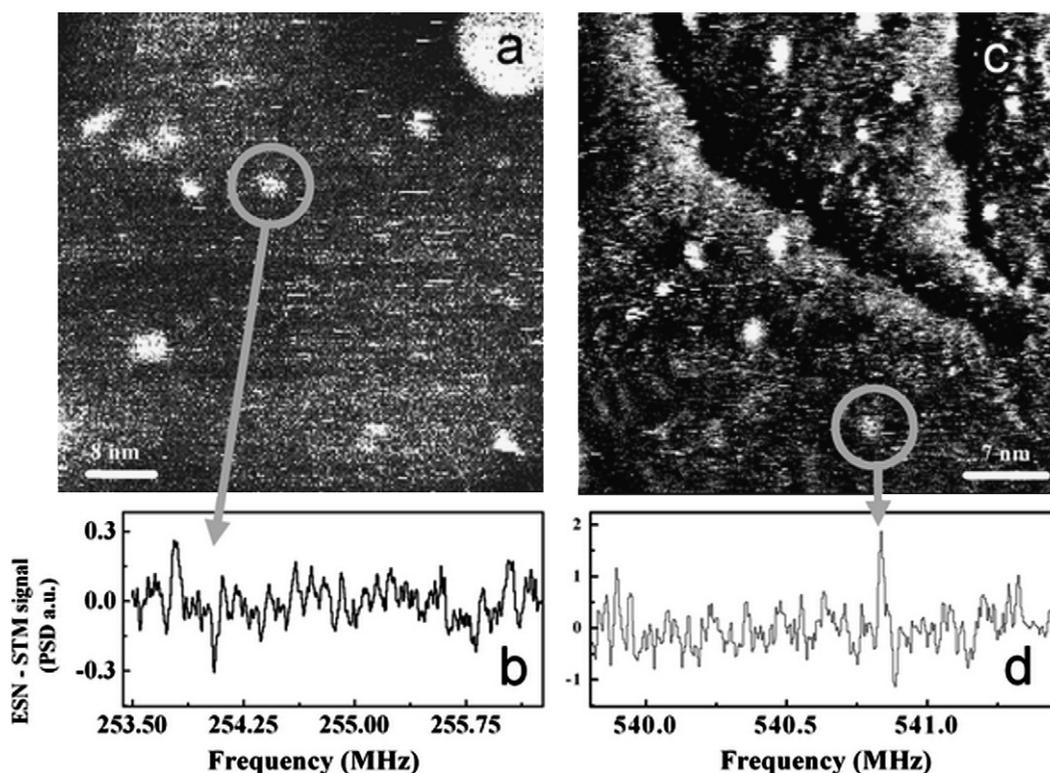
Fig. 4. (a) STM image of DPPH molecules and aggregates during ESN-STM measurement. (b) ESN-STM spectrum of a DPPH molecule deposited on Au(1 1 1), indicated by an arrow in (a). (c) STM image of DPPH molecules on Au(1 1 1) observed in a different region of the sample and (d) ESN-STM spectrum of a single DPPH molecule, evidenced by an arrow in (c), with increased S/N ratio. The ESN-STM spectra were acquired with AC modulation frequency and intensity of 16 kHz and 13 mG, respectively.

The ESN-STM investigation on DPPH molecules evidenced a peak whose frequency varied with the applied magnetic field. The signal presented in Fig. 4b is observed when the STM tip is localized on the molecule of Fig. 4a at a frequency of 254 MHz which for $g = 2.0$ corresponds, within the error bar, to the measured applied DC magnetic field of 91 ± 1.5 G. In Fig. 4c a peak at higher field is reported. A bias voltage of 50 mV and 30 pA of tunnelling current were used as imaging parameter whereas during spectroscopy the current was raised to 1 nA. When a peak appeared in the spectrum the position of the tip was always localized on a single molecule.

We note that for the lowest frequency peak the expected derivative lineshape is not observed; we suppose that this signal distortion might be induced by a value of the modulation amplitude lower than the optimal one [5a]. To clarify this point further experiments are planned in the next future.

In order to prove that the observed peak is due to a spin dependent phenomenon, DC magnetic field has been varied. The theoretical linear dependence of the Larmor frequency with the magnetic field has been verified as shown in Fig. 5.

It has to be noted that we explored only the central region of the expected five lines hyperfine structure of DPPH due to present limitations of our instrumental setup. Further investigation and upgrading of the experimental setup are currently in progress. In particular, our main
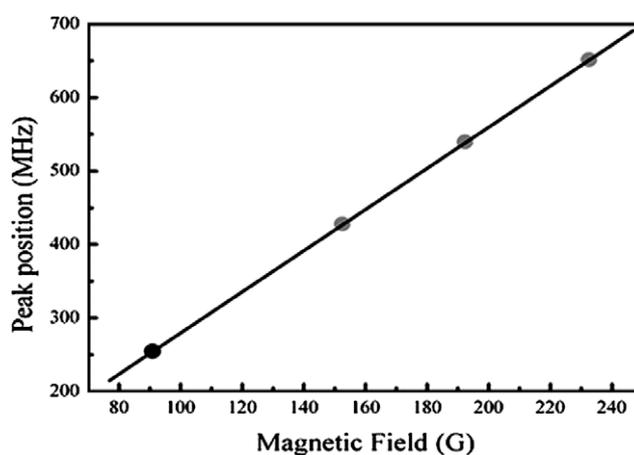

Fig. 5. Position of ESN-STM peak measured at different values of applied magnetic field. Points above 400 MHz were reported in Ref. [4]. The slope of the best fit line is $g\mu_B/h$: the obtained value for g is equal, within experimental error, to 2.0.

effort is directed to improve the sensitivity of the RF detector, by adding a tuning circuit and improving the impedance matching between source and amplifier.

6. Establishing a characterization protocol for new samples

In order to improve the homogeneity, the stability and the degree of organization of the investigated samples,
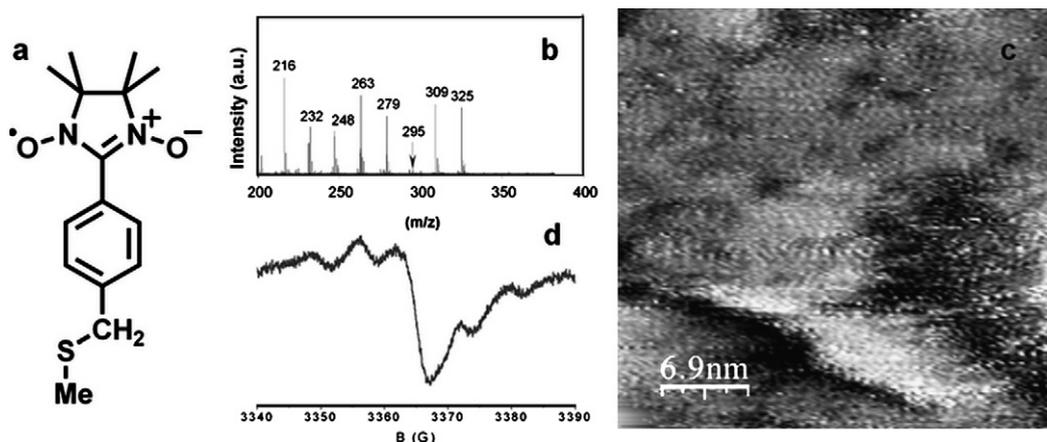
Fig. 6. (a) The structure of one of the investigated radicals, (b) ToF-SIMS positive spectra, (c) STM image and (d) CW-ESR spectrum of a self-assembled monolayer of the radical shown in (a). Adapted from Ref. [14].

we suggest now to exploit the well known properties of self-assembled monolayers (SAMs) [8]. This approach relies on the use of functional groups capable to bind specific surfaces and to form a bidimensional lattice of molecules. The 2D-organization results from inter-molecular lateral interactions. Moreover, specific substituents can be added to such molecules in order to obtain completely or partially functionalized monolayers of selected molecules. For our purpose the desired "function" is a paramagnetic center, and in particular we oriented our interest towards nitronyl nitroxides radicals (NitRs). These are a class of paramagnetic compounds [10], widely studied both for their intrinsically interesting magnetic properties as purely organic bulk ferromagnets [11] and as building blocks for assembling complex magnetic structures in which they act as chemical and magnetic linkers between transition metals [12], to yield magnetic polymers [13].

We have shown elsewhere [14] how it is possible to prepare and obtain a complete characterization of the deposed monolayers of this kind of paramagnetic molecules. This includes a chemical characterization through ToF-SIMS technique, a morphological characterization through STM measurement and magnetic characterization of the monolayers through CW-ESR spectroscopy. In our opinion this is the best starting point toward local ESN-STM investigations of single molecules. Indeed we feel that a deeper knowledge of the characteristics of the sample to be investigated by ESN-STM might increase the probability of a successful measurement. All NitRs utilized were specifically sensitized in order to contain suitable linking groups for the gold surface, usually a thioether group linked in para- position of a phenyl- substituted NitR. Here we summarize the results obtained with one of these NitRs, namely *p*-benzyl-*S*-methyl-nitronyl-nitroxide (NitPhCH$_2$-SMe, see Fig. 6a), which presented the best self-assembling characteristics. Detailed synthesis and descriptions of the characterizations can be found elsewhere [14].

The deposition of this radical achieves a molecular scale ordering: chemically specific interactions between molecular linking group and surface avoid the formation of multilayers and small clusters observed using BDPA [3a,4] or DPPH [4]. The deposition is obtained by soaking flame-annealed Au(111) substrates in 1–2 mM solutions in CH$_2$Cl$_2$ of NitRs. The slides are incubated in the dark at 60 °C overnight and then rinsed with anhydrous CH$_2$Cl$_2$ and dried with nitrogen flux.

ToF-SIMS spectra (Fig. 6b) recorded on deposited samples showed the presence of the molecular peak, thus suggesting that molecules adsorb unaltered on surfaces. On the other hand, STM investigation[1] gave evidence for the actual presence of self-assembled monolayers (Fig. 6c). Further it indicates that deposition results in regions of locally ordered monolayers and suggests a possible binding mode for the radical on the surface. Finally, X-band ESR spectra (Fig. 6d) showed the persistence of the paramagnetism of the molecules and the five line hyperfine structure indicates the presence of the "Nit" function. No angular dependence of the spectra was observed and this was attributed [14] to the absence of long range order. This result is not in contradiction with STM evidences: indeed both the intrinsic mobility of the radical heads and the presence of domains of different orientations on gold surface (observed also in the STM image) result in the averaging of the anisotropies. This set of results is summarized in Fig. 6. It is to be outlined that all the analyses were performed on samples prepared following the same procedure. We believe that the film characterization procedure described above is an effective protocol for achieving appropriate samples for the ESN-STM experiments.

---

[1] This STM image has been obtained with an NT-MDT P47pro STM at room temperature with Pt/Ir mechanically etched tips as described in Ref. [14].
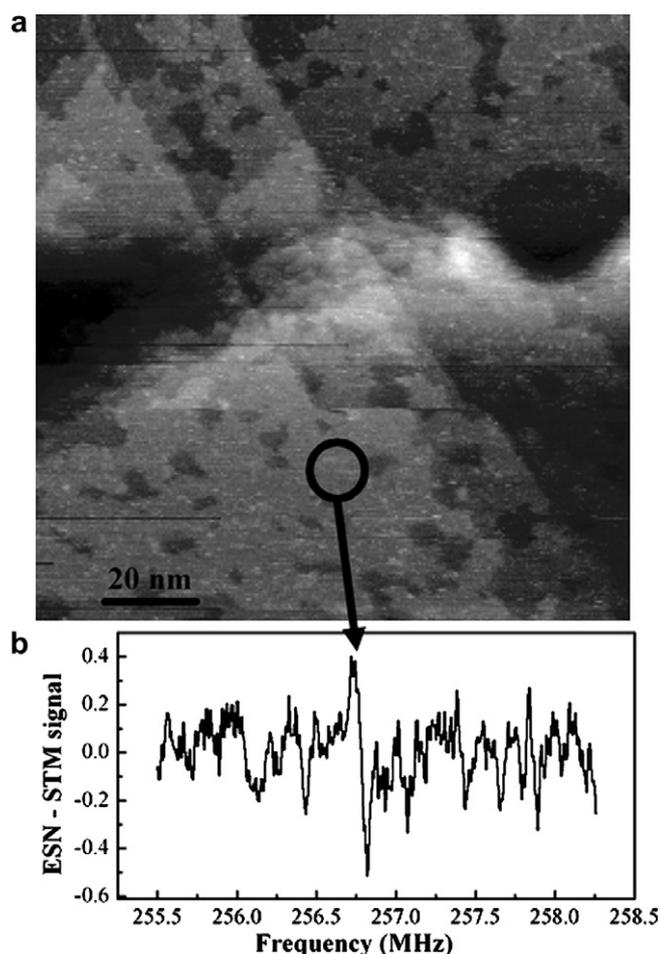
Fig. 7. STM image (a) and corresponding ESN-STM spectrum (b) of the self-assembled monolayers of radical presented in Fig. 6. The spectrum was taken in the zone marked with the circle. Experimental conditions during STM imaging: $I_t = 30$ pA, BV = 0.1 V. The parameters during ESN-STM measurement were $I_t = 1$ nA, BV = 50 mV, AC modulation frequency and intensity: 16 kHz, 13 mG.

Very recently, we started the investigation of this kind of samples using ESN-STM. Preliminary and not conclusive observation suggests that these samples give a signal above the noise level, with a seemingly increased reproducibility and detectability of the signal due to the increased quality of the samples. More experimental evidences need to be gathered in order to reach a definite conclusion. In Fig. 7b the first observation of a signal originated from a NitPhCH$_2$SMe molecule is presented. We note here that the resolution quality of the topography presented in Fig. 7a, and obtained with our home-made ESN-STM is lower than the commercial standard STM used for Fig. 6c, and only reveals the presence of monolayer features like pinholes (the darker spots in Fig. 7a). However the physico-chemical characterization described above provides convincing evidences that ESN-STM measurements are performed on monolayers, and thus of the single molecular character of the reported spectra.

7. Conclusion

Our efforts in single spins investigation through ESN-STM technique were summarized. We presented the description of our home built apparatus and first measurements on surface deposited DPPH. Finally, using a nitronyl-nitroxide derivative, we described a complete characterization protocol for assessing the quality and the properties of molecular based paramagnetic films before ESN-STM investigations.

Acknowledgements

References

[1] (a) D. Rugar, R. Budakian, H.J. Mamin, B.W. Chui, Nature 430 (2004) 329;
(b) J.M. Elzerman, P. Hanson, L.H. Willems van Beveren, B. Witkamp, L.M.K. Vandersypen, L.P. Kouwenhoven, Nature 430 (2004) 431;
(c) M. Xiao, I. Martin, E. Yablonovitch, H.W. Jiang, Nature 430 (2004) 435;
(d) A.J. Heinrich, J.A. Gupta, C.P. Lutz, D.M. Eigler, Science 306 (2004) 466.
[2] Y. Manassen, R.J. Hamers, J.E. Demuth, A.J. Castellano, Phys. Rev. Lett. 62 (1989) 2531.
[3] (a) C. Durkan, M.E. Welland, Appl. Phys. Lett. 80 (2002) 458;
(b) C. Durkan, Contemp. Phys. 45 (2004) 1.
[4] P. Messina, M. Mannini, A. Caneschi, D. Gatteschi, L. Sorace, P. Sigalotti, C. Sandrin, P. Pittana, Y. Manassen, J. Appl. Phys., in press, doi:10.1063/1.2434832.
[5] (a) Y. Manassen, J. Magn. Reson. 126 (1997) 133;
(b) Y. Manassen, I. Mukhopadhyay, N. Ramesh Rao, Phys. Rev. B 61 (2000) 16223.
[6] A.V. Balatsky, Y. Manassen, R. Salem, Phil. Mag. B 82 (2002) 1291.
[7] T. Sleator, E.L. Hahn, C. Hilbert, J. Clarke, Phys. Rev. Lett. 55 (1985) 1742.
[8] A. Ulman, Ultrathin Organic Films, Academic Press Inc., San Diego, CA, 1991.
[9] (a) A. Abragam, B. Bleaney, Electron Paramagnetic Resonance of Transition Ions, Dover Publications, New York, 1986;
(b) J.P. Goldsborough, M. Mandel, G.E. Pake, Phys. Rev. Lett. 4 (1960) 13;
(c) J.P. Lloyd, G.E. Pake, Phys. Rev. 92 (1953) 1576.
[10] J.H. Osiecki, E.F. Ullman, J. Am. Chem. Soc. 90 (1968) 1078.
[11] (a) M. Tamura, Y. Nakazawa, D. Shiomi, Y. Nozawa, M. Hosokoshi, M. Ishikawa, M. Kinoshita, Chem. Phys. Lett. 186 (1991) 401;
(b) R. Chiarelli, M.A. Novak, A. Rassat, J.L. Tholence, Nature 363 (1993) 147.
[12] A. Caneschi, D. Gatteschi, R. Sessoli, P. Rey, Acc. Chem. Res. 22 (1989) 392.
[13] A. Caneschi, D. Gatteschi, N. Lalioti, C. Sangregorio, R. Sessoli, G. Venturi, A. Vindigni, A. Rettori, M.G. Pini, M.A. Novak, Angew. Chem., Int. Ed. Engl. 40 (2001) 1760.
[14] M. Mannini, L. Sorace, L. Gorini, F.M. Piras, A. Caneschi, A. Magnani, S. Menichetti, D. Gatteschi, Langmuir 23 (2007) 2389.